Toxicology and Applied Pharmacology 437 (2022) 115886

Contents lists available at ScienceDirect

Toxicology and Applied Pharmacology

journal homepage: www.elsevier.com/locate/taap

Kinase inhibitor-induced cardiotoxicity assessed in vitro with human pluripotent stem cell derived cardiomyocytes

Hai-Qing Xian [a], Carmina Blanco [b], Kristina Bonham [a], H. Ralph Snodgrass [a,*]

[a] VistaGen Therapeutics, Inc., 343 Allerton Ave., South San Francisco, CA, 94080, United States of America
[b] Senti Biosciences, 2 Corporate Drive, South San Francisco, CA 94080, United States of America

ARTICLE INFO

Keywords:
Cardiotoxicity
Human pluripotent stem cells
hPSC
Cardiomyocytes
Kinase inhibitors
MEA

ABSTRACT

Many small molecule kinase inhibitors (SMKIs), used predominantly in cancer therapy, have been implicated in serious clinical cardiac adverse events, which means that traditional preclinical drug development assays were not sufficient for identifying these cardiac liabilities. To improve clinical cardiac safety predictions, the effects of SMKIs targeting many different signaling pathways were studied using human pluripotent stem cell derived cardiomyocytes (hPSC-CMs) in combined assays designed for the detection of both electrophysiological (proarrhythmic) and non-electrophysiological (non-proarrhythmic) drug-induced cardiotoxicity. Several microplate-based assays were used to quantitate cell death, apoptosis, mitochondrial damage, energy depletion, and oxidative stress as mechanism-based non-electrophysiological cardiomyocyte toxicities. Microelectrode arrays (MEA) were used to quantitate in vitro arrhythmic events (iAEs), field potential duration (FPD) prolongation, and spike amplitude suppression (SAS) as electrophysiological effects. To enhance the clinical relevance, SMKI-induced cardiotoxicities were compared by converting drug concentrations into multiples of reported clinical maximum therapeutic plasma concentration, "FoldC_{max}", for each assay. The results support the conclusion that the combination of the hPSC-CM based electrophysiological and non-electrophysiological assays have significantly more predictive value than either assay alone and significantly more than the current FDA-recommended hERG assay. In addition, the combination of these assays provided mechanistic information relevant to cardiomyocyte toxicities, thus providing valuable information on potential drug-induced cardiotoxicities early in drug development prior to animal and clinical testing. We believe that this early information will be helpful to guide the development of safer and more cost-effective drugs.

1. Introduction

Small molecule kinase inhibitors (SMKIs) have revolutionized cancer therapy due to their targeted effects and decreased systemic toxicity, as compared to many classic cancer drugs. By 2020, the FDA had approved 49 SMKIs for cancer therapy (Lamore et al., 2020). However, several studies have revealed that some SMKIs cause unanticipated serious adverse cardiac effects in patients (Kenigsberg et al., 2016; Lamore et al., 2020), including left ventricular dysfunction (LVD), cardiomyopathy, heart failure (HF), QT prolongation, and Torsades de Pointes (TdP) (Woosley et al., 2021). Many of these SMKI-induced cardiac toxicities failed to be detected during preclinical drug development due to the limitations of current cardiotoxicity screening methods.

Cardiotoxicities are caused by multiple mechanisms. Drug-induced QT prolongation and TdP are due to cardiac electrophysiological effects. We define this type of proarrhythmic effect as "electrophysiological cardiotoxicity" in these studies. On the other hand, non-proarrhythmic toxicities, such as cardiomyopathy and heart failure, can result in alterations in metabolism, transporters, structural changes, and the interrelationship between vascular biology and cardiac structural changes due to drug treatment. These serious effects can lead to damage or death of cardiomyocytes (CMs) (Laverty et al., 2011). Herein, we refer to these as "non-electrophysiological cardiotoxicities." Current U.S. Food and Drug Administration (FDA)-mandated drug safety guidelines (FDA, 2001, 2005) recommending hERG assay analysis, primarily focus on prevention of drug-induced TdP risks, but this assay does not provide any information on non-electrophysiological cardiotoxicities. To date, there are no FDA-recommended in vitro assays for detecting non-electrophysiological cardiotoxicities. As a result, drug-induced severe adverse events, such as cardiomyopathy and heart

* Corresponding author.
E-mail address: rsnodgrass@vistagen.com (H.R. Snodgrass).

https://doi.org/10.1016/j.taap.2022.115886
Received 2 September 2021; Received in revised form 4 January 2022; Accepted 10 January 2022
Available online 15 January 2022

failure, can go undetected at early stages of drug development. Not being able to detect these potential cardiotoxicities prior to clinical trials increases the risk of late-stage termination of drug development programs, e.g., tozasertib (Durlacher et al., 2016; Green et al., 2011), or a potential post-approval market withdrawal, e.g., ponatinib (FDA, 2013; Talbert et al., 2015).

Therefore, efficient preclinical assessment of a wide range of cardiac liabilities should not be restricted to limited electrophysiological analyses, such as hERG assays. A more comprehensive preclinical assessment of both the electrophysiological and non-electrophysiological aspects of cardiac cell biology should be considered for drug safety evaluation prior to clinical studies.

There has been some progress in the field toward expanding cardiac toxicity assessment beyond electrophysiological studies. Image analysis-based hPSC-CM assays for assessing drug-effects on general CM health have been explored by several groups (Clements et al., 2015; Doherty et al., 2013; Pointon et al., 2013; Thomas, 2012). However, these studies require expensive equipment, sophisticated image analysis software, and large data handling, which can limit throughput. Furthermore, consistency and reproducibility of high content imaging assays need to be thoroughly examined, as it is common for variables that would not be noticeable in traditional assays to become a major source of variance (William Buchser et al., 2014). To address these limitations, we aim to develop non-image-based assays that increase the throughput and predictiveness for assessing non-electrophysiological cardiotoxicities that are associated with damage and death of CMs, as well as examine underlying functional mechanisms of toxicity.

A non-image based cell viability assay using hPSC-CMs for assessing cardiac toxicity of tyrosine kinase inhibitors was reported, however, the underlying mechanisms of cardiotoxicity were not investigated (Sharma et al., 2017). Apoptosis is an important pathway that results in CM death and subsequently leads to cardiac impairment such as HF (Wencker et al., 2003). In addition, mitochondrial dysfunction is implicated in LVD and HF (Lamore et al., 2020). The mitochondrial role in cellular energy production is critical to cardiac function of the ATP-regulated contraction–relaxation cycle within the myocardium (Brown et al., 2017). Finally, oxidative stress leads to multiple adverse effects, such as energy imbalance, mitochondrial dysfunction, and activation of stress-related signaling pathways (Deavall et al., 2012). Because these pathways are critical to cardiac function, we sought to extend the evaluation of drug effects on CM health by gaining insight into mechanistic aspects of non-electrophysiological cardiotoxicity, such as apoptosis, mitochondrial dysfunction, oxidative stress, and energy metabolism disruption, with high throughput microplate-based assays.

The standard FDA-recommended hERG assays that are used for preclinical assessment of drug-induced arrhythmogenesis, although useful, have several limitations. For example, they are based on non-human, non-CM systems that express only the single hERG ion channel (FDA, 2001) out of many ion channels that are critical to cardiac function. Moreover, hERG binding assays can yield both false positive and false negative predictions (Johannesen et al., 2014), especially since hERG assays are not sensitive to: 1) drug effects on the protein processing and functional expression of the hERG ion channel; 2) multi-ion channel counterbalancing drug effects (Nogawa and Kawai, 2014); or 3) toxic drugs that do not affect cardiac electrophysiology (Nogawa and Kawai, 2014).

To improve predictivity of proarrhythmic risk of drug candidates at an early stage of development, many different approaches have been explored, namely in silico modeling for reconstructions of cellular cardiac electrophysiologic activity and hPSC-CM based electrophysiological assays. Human-based in silico models are emerging as important tools to study the effects of integrating multiple ion channel currents to predict clinical proarrhythmic risk (Hwang et al., 2020; Lancaster and Sobie, 2016; Strauss et al., 2019; Valerio Jr. et al., 2013). In general, these approaches use drug-specific quantitative data for individual ion channels as the inputs for computationally intensive mechanistic models to develop simulated multichannel drug effects on cardiac physiology. Under the Comprehensive in vitro Proarrhythmia Assay (CiPA) initiative, a consensus in silico model has been developed with the in vitro data of seven ionic currents to reconstruct cellular electrophysiologic activity to assess the risk of cardiotoxicity (Park et al., 2019; Strauss et al., 2019). The latest validation studies suggest that the hPSC-CM assays can be useful when combined with other in silico strategies (Park et al., 2019).

Using hPSC-CMs as a model system for developing preclinical assays to detect drug-induced cardiotoxicity is of great interest, as large numbers of hPSCs, representing many different genetic backgrounds and disease states, are either available or can be produced, and these can be differentiated into CMs that exhibit molecular and functional properties of human myocardial cells (Davila et al., 2004; Germanguz et al., 2011; Yang et al., 2008). Importantly, these cellular models contain the full complement of human cardiac ion channels. While several groups (Blinova et al., 2018; Guo et al., 2013; Peng et al., 2010) have shown applications of hPSC-CM assays for predicting proarrhythmic risk of drug candidates using platforms such as MEA, FLIPR, impedance, xCELLigene RTCA, CardioECR, and CellOPTIQ (Lamore et al., 2020), hPSC-CM based MEA assays have been explored for assessing drug-induced electrophysiological alterations since 2008 (Yang et al., 2008). In recent years, MEA assays for proarrhythmic risk analyses were validated mainly with panels of non-SMKI drugs in various studies including the studies under the CiPA initiative (Ando et al., 2017; Blinova et al., 2018). Here, we extend the application of MEA assays to testing SMKI-induced electrophysiological drug effects.

With both the non-electrophysiological and electrophysiological hPSC-CM assays, along with optimized analytical processes, we generated mechanistically broad cardiotoxicity profiles for a panel of 18 selected SMKIs that target different signaling pathways. The results were highly concordant with reported non-electrophysiological and electrophysiological clinical adverse events.

2. Materials and methods

2.1. hPSC maintenance and cardiac differentiation

All StemPro-34 media and supplements were purchased from Life Technologies Corporation, unless otherwise stated. Growth factors were purchased from R&D Systems. HES-2 (ESIBIe002-A) human embryonic stem cells (hESCs) were purchased from BioTime and subsequently trypsin-adapted. hESCs were maintained on MEFs (Applied StemCell Inc.) at 80–90% confluency in hESC Maintenance Medium supplemented with 20% Knockout serum replacement (Kennedy et al., 2007), except antibiotics were omitted and 1.4 mM L-glutamine was used. The differentiation protocol for generating hPSC-CMs (Supplemental Fig. S1) was adapted and modified from published protocols (Yang et al., 2008; Zhang et al., 2013). Briefly, hESCs were replated onto growth factor reduced Matrigel (Corning) coated plates in hESC Maintenance Medium containing 20 ng/ml bFGF for 2 days. Cells were then differentiated in low-attachment plates as embryoid bodies (EBs) in a Basal Medium of StemPro-34 medium supplemented with L-glutamine (2 mM), transferrin (150 μg/ml, Roche), ascorbic acid (50 μg/ml), and monothioglycerol (0.45 mM). Growth factors and small molecule compounds were added to the Basal Medium sequentially as follows: day 1, BMP4 (0.5 ng/ml); days 2–4, bFGF (5 ng/ml), activin A (6 ng/ml), and BMP4 (10 ng/ml)); days 5–6, VEGF (10 ng/ml), Wnt-C59 (2 μM, Cellagen Tech.), and dorsomorphin (0.5 μM, Sigma); and days 7–8, VEGF (10 ng/ml) and Wnt-C59 (2 μM). From day 8 to day 20, the medium was exchanged every 3 days with VEGF (10 ng/ml) and bFGF (5 ng/ml). After day 20, the medium was replaced with 5% FBS in DMEM every 3 days. For the first 12 days of differentiation, EBs were cultured in a hypoxic environment (5% CO_2, 5% O_2). Afterwards, EBs were cultured in an ambient oxygen environment (5% CO_2, 21% O_2).

2.2. Flow cytometry

On day 20 of cardiac differentiation, cardiac cell clusters were dissociated to a single cell suspension using 0.1% collagenase type II (Worthington) at 37 °C for 1 h, followed by 0.25% trypsin/EDTA at 37 °C for 5–10 min. Single cells were fixed with 2% PFA for 10 min and then stained with FITC-labeled cTnT antibody (abcam; Cat #: ab105439; Dilution: 1:200) for 1 h on ice. A BD Accuri™ C6 Flow Cytometer was used for analysis.

2.3. Compounds

Axitinib, sunitinib malate, temsirolimus, and DMSO (cell culture grade) were purchased from Sigma-Aldrich. Alvocidib, barasertib, selumetinib, and XL765 were purchased from Selleck Chem. Other kinase inhibitors (dasatinib, erlotinib, everolimus, imatinib [methanesulfonate salt], lapatinib [di-p-toluenesulfonate salt], lestaurtinib, nilotinib, perifosine, PD325901, sorafenib [p-toluenesulfonate salt], and tozasertib) were purchased from LC Laboratories. The purity of all compounds was 98% or greater. All compounds were reconstituted in 100% DMSO at 20–50 μM and stored at -80 °C until used.

2.4. hPSC-CM based Non-Electrophysiological Toxicity (NET) assays

hPSC-derived cardiac cell clusters were dissociated into a single cell suspension using 0.1% collagenase type II (Worthington) at 37 °C overnight, followed by 0.25% trypsin/EDTA (Corning) at 37 °C for 5–10 min. Single cells were plated in 384-well plates that had been pre-coated with 10 μg/ml fibronectin (Sigma). The cells were seeded at 7000 cells per well in a volume of 25 μl of DMEM supplemented with 20% FBS (Invitrogen). After one day, the medium was switched to DMEM with 2% FBS and cultured for 4 days. On the drug testing day, compounds from DMSO stocks were diluted in phenol red-free DMEM containing 2% FBS. The final concentration of DMSO was 0.5% in all drug dilutions. After all the medium was removed from each well, 25 ul of diluted compound was added to each well. Each drug concentration was tested in replicates of four wells.

To measure cell viability, the cells were treated with drugs for 72 h and then assayed with CellTiter Blue (Promega). To measure oxidative stress, apoptosis, or mitochondria membrane potential, the cells were treated with compounds for 18 h and then assayed with GSH-Glo (Promega), Caspase3/7-Glo (Promega), or JC-10 (AAT Bioquest), respectively. To measure energy depletion, the cells were treated with drugs for 48 h and then analyzed with ATP-Glo (Promega). Assays were performed according to manufacturers' instructions and analyzed with a Tecan Safire II plate reader for fluorescence and luminescence readings.

2.5. hPSC-CM based MEA assays

A Maestro MEA system with AxIS software (Axion Biosystems) was used for recording electrophysiological activities of hPSC-CMs treated with SMKIs. First, CM clusters were dissociated into single cells with the same procedure as above and then plated onto Matrigel-coated MEA plates at 3–3.75 $\times$ 10^4 cells per well. After the cells were cultured in 20% FBS/DMEM for one day, the medium was switched to 5% FBS/DMEM and exchanged every 2–3 days until the cells were ready for drug testing, as defined by a spike amplitude greater than 1 mV. This typically took 8–10 days post cell plating.

On the drug testing day, compounds were diluted from DMSO stocks into secondary drug stocks using DMEM containing 2% FBS. Before drug testing, cells were first equilibrated in Recording Medium (RM), which contained 2% FBS and 0.48% DMSO in DMEM, at 37 °C with 5% CO_2 for at least an hour. Baseline recordings were then taken with the AxIS software on a Maestro MEA system according to the manufacturer's instructions. Subsequently, a test drug was added to each well by substituting 1/3 media volume with the lowest concentration secondary drug stock (3 μM) in RM, and a one-hour MEA recording was made in the same manner as the baseline recording. This dilution and recording sequence was sequentially repeated twice in the same well using increasingly higher secondary stock solutions of the drug (24 μM and 72 μM, respectively) in RM. For the final drug concentration, each well received a full volume RM exchange with the highest drug concentration (72 μM). This approach yielded triplicate wells of four final testing concentrations (1, 8.7, 30 and 72 μM) of each drug, with constant DMSO concentrations of 0.48%, for MEA analyses. For DMSO background and process-related controls, every MEA plate had three wells of RM with DMSO (0.48%) that went through the same process as the drug groups.

2.6. Data analysis for NET assays

For the five cardiac NET assays, experimental data were analyzed and reported as mean ± STDV. For easy comparison of multiple SMKIs across multiple assays, a heatmap format was adopted, with drug effects divided into quartiles for each assay and the maximum measured effect defined as 100%. To categorize drug-induced non-electrophysiological cardiac effects, the IC_{50} or EC_{50} values of each drug in each assay was calculated with dose response curves done in GraphPad Prism. To provide more clinical relevance, the IC_{50} or EC_{50} values were converted to multiples of reported clinical maximum therapeutic plasma concentration, C_{max}, for each drug and expressed as "FoldC_{max}". See Supplemental Table S1 for drug specific clinical C_{max} values.

Using FoldC_{max} values, the drug effects were classified into four levels of CM toxicity: 1) no obvious toxicity observed; 2) low toxicity, >300 FoldC_{max}; 3) moderate toxicity, 30 to 300 FoldC_{max}; and 4) significant toxicity, <30 FoldC_{max}.

2.7. Data analysis for MEA assays

MEA raw recordings of cardiac electrophysiological activities were batch-analyzed with AxIS software (Axion BioSystems). Three main parameters, drug-induced in vitro arrhythmic events (iAEs), field potential duration (FPD), and spike amplitude suppression (SAS), were further analyzed with the Cardiac Analysis Tool (Axion BioSystems) according to the manufacturer's instructions. iAEs marked in the Cardiac Analysis Tool were further confirmed manually by inspecting the AxIS waveform tracings. FPD measurements were corrected using Fridericia's rate correction algorithm (FPDc) (Fridericia, 2003). The FPDc and spike amplitude of each experimental group were normalized by subtracting the DMSO control on the same MEA plate. After normalization, drug effects and baseline effects in each condition were averaged among triplicate wells to calculate the percentage change of drug effects. Percentage change = (drug effects - baseline effects) / baseline effects. FPDc effects can be either reduction or prolongation, and FPDc prolongation can be more than 100%. However, the maximum SAS effect is 100%, which indicates spontaneous beating was completely suppressed. For iAEs, if one of three wells showed iAEs after drug treatment, that compound was recorded as having a 33% iAE effect. If all wells showed iAEs, then the compound was recorded as having a 100% iAE effect. When beats were either not detected, i.e. quiescent wells (Q), or when the beats were present but below threshold detection, the FPD was not measurable, and SAS was recorded as 100%. Arrhythmic events were not measurable in quiescent wells, and therefore they were not included for calculation of percentage of iAE effect.

For an easy visual comparison of drug effects, the percentage change of drug-induced iAEs, FPDc change, and SAS were plotted in heatmaps with the darkest shade for the greatest percentage effect in each assay. SMKI-induced iAEs were divided into four levels (0%, 33%, 66%, and 100%). FPDc effects were classified into six levels (<−15%, ±15%, 16–30%, 31–60%, 61–100%, and > 100%). SAS effects were classified into five levels (<25%, 25–50%, 51–75%, >76%, and Q).

To assess assay results at clinically relevant drug concentrations, we estimated iAE_{33}, $FPDcP_{30}$, and SAS_{30} and converted those values to

"FoldC_{max}", which were used for toxicity ranking. iAE_{33} is defined as the drug concentration that caused iAEs in 33% of wells. $FPDcP_{30}$ is defined as the drug concentration that prolonged FPDc by 30% compared to its baseline. SAS_{30} is defined as the drug concentration that suppressed spike amplitude by 30% compared to its baseline.

Based on FoldC_{max} values of iAE_{33}, SMKIs were divided into four iAE categories: 1) no iAEs; 2) minimal (iAEs >100 FoldC_{max}); 3) moderate (iAEs between 10 and 100 FoldC_{max}); and 4) severe (iAEs <10 FoldC_{max}). Using FoldC_{max} values of $FPDcP_{30}$, SMKIs were classified into five FPDc categories: 1) a reduction of FPDc; 2) insignificant effect at any concentration (±15% FPDc change); 3) mild effects ($FPDcP_{30}$ > 50 FoldC_{max}); 4) moderate effects ($FPDcP_{30}$ between 5 and 50 FoldC_{max}); and 5) severe effects ($FPDcP_{30}$ < 5 FoldC_{max}). With FoldC_{max} values of SAS_{30}, SMKIs were grouped into four SAS categories: 1) no SAS; 2)

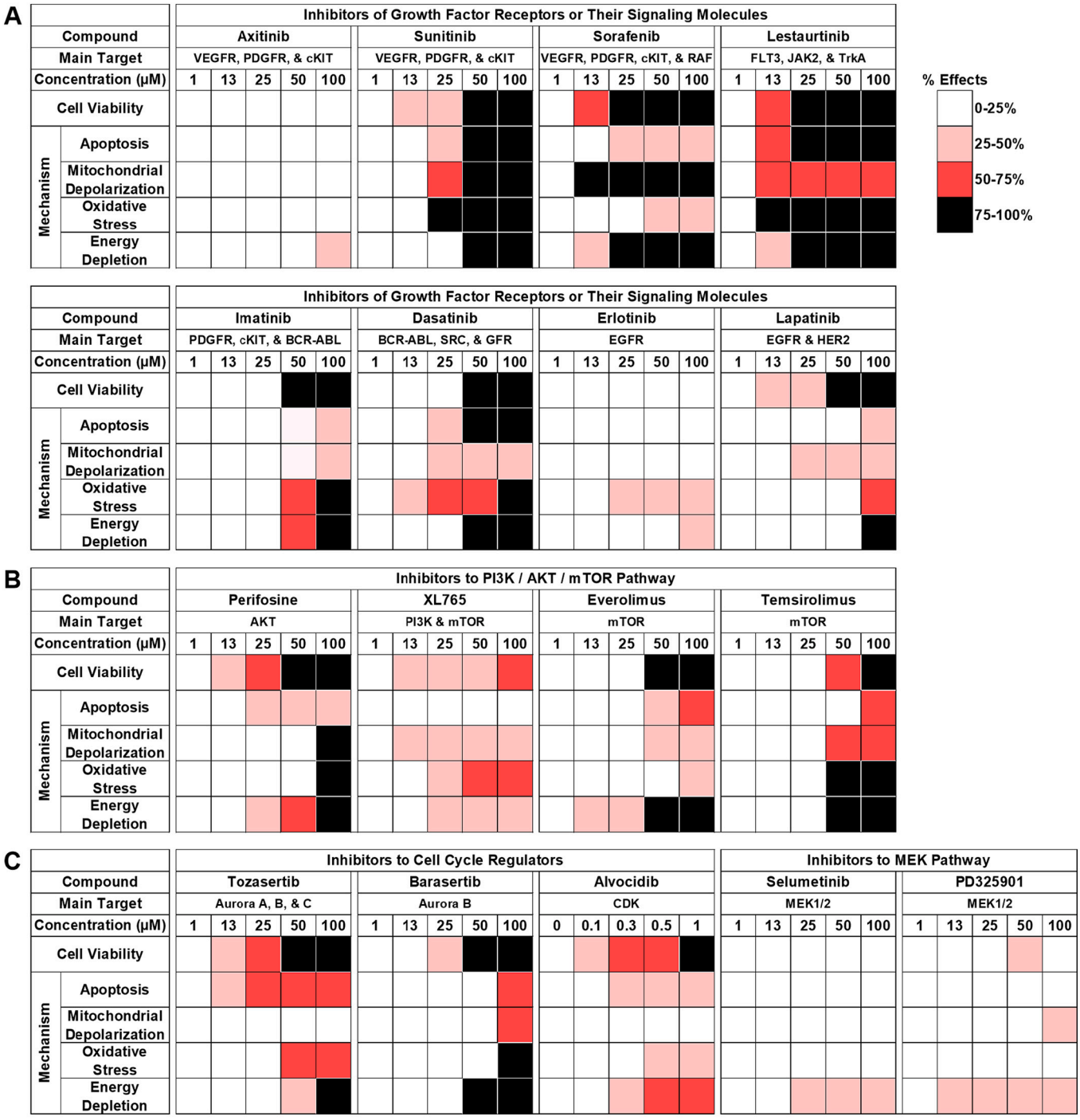

Fig. 1. In vitro Assessment of Non-Electrophysiological Cardiac Toxicity of SMKIs in hPSC-CMs.
SMKIs targeting different signaling pathways were tested in five NET assays. The Cell Viability Assay measures drug-induced total cardiomyocyte death, while the four mechanistic assays detect potential mechanisms affecting cardiomyocyte viability. Average drug effects of quadruplicate wells at each concentration were plotted for each assay in a heatmap format, with drug effects divided into quartiles. 100% is defined as the maximum measured effect. **A)** SMKIs that target different growth factor receptors or their signaling molecules. **B)** SMKIs that target the PI3K/AKT/mTOR pathway. **C)** SMKIs that target cell cycle regulators or the MEK pathway.

minimal (SAS >100 FoldC_{max}); 3) moderate (SAS between 10 and 100 FoldC_{max}); and 4) severe (SAS <10 FoldC_{max}).

3. Results

3.1. SMKIs induce non-electrophysiological toxicity in hPSC-CMs

To analyze drug-induced non-electrophysiological toxicity (NET), a panel of five NET assays were developed to quantitate drug-induced CM death, apoptosis, mitochondrial membrane depolarization, oxidative stress, and energy metabolism disruption using hPSC-CMs, which express all the major ion channel genes and various cardiac markers (Supplemental Fig. S1). The first NET assay measures loss of cell viability after prolonged drug treatment. The other four NET assays are designed to investigate distinct mechanistic pathways of CM dysfunction that ultimately could lead to cell death.

NET assays were validated with 17 SMKIs, which target many different signaling pathways and show different degrees of cardiotoxicity. Dose response curves are presented in Supplemental Figs. S2-S6. For an easy comparison of different compounds across all NET assays, the results were plotted in a heatmap format, which provides a visual highlight of the unique cardiotoxicity profile of each compound and points to potential differences between mechanisms of toxicity (Fig. 1).

These NET assays revealed different cardiac toxicity profiles for eight SMKIs targeting growth factor receptors or their signaling molecules (Fig. 1A). Although axitinib, sunitinib, and sorafenib all target VEGFR, PDGFR, and cKIT, it has been reported that sunitinib and sorafenib cause multiple types of adverse cardiac events in patients, while axitinib is rarely associated with cardiotoxicity (FDA, 2012) (Supplemental Table S1). Consistent with these clinical observations, sunitinib and sorafenib have serious effects in the NET assays, whereas axitinib has little effect in any of these assays (Fig. 1A). Although both sunitinib and sorafenib were toxic to hPSC-CMs, they triggered different mechanistic pathways. Sunitinib induced all four mechanisms of toxicity, but sorafenib predominantly induced mitochondrial toxicity and depleted energy in hPSC-CMs. Lestaurtinib is a promiscuous SMKI that inhibits many kinase pathways, including JAK2, FLT3, and TrkA (Mosquera Orgueira et al., 2020). It exhibits significant toxicity in all NET assays; however, mitochondrial depolarization does appear to be somewhat less severe than the other four mechanisms of toxicity (Fig. 1A). The predicted lestaurtinib-induced cardiotoxicity in the NET assays is consistent with clinical reports of its cardiac liabilities (Supplemental Table S1).

Likewise, imatinib and dasatinib, which bind to PDGFR, cKIT, BCR-ABL, SRC, or GFR, are associated with known clinical cardiac liabilities (Supplemental Table S1). Consistently, both SMKIs induced CM toxicity in the NET assays and demonstrate the utility of the NET assays to provide potential mechanistic insight into drug-induced cardiotoxicity. This applies to SMKIs that inhibit other growth factor receptor pathways as well. For example, whereas dasatinib demonstrates toxicity in all the mechanistic pathways, imatinib-related toxicity mainly involves oxidative stress and energy depletion pathways, despite both drugs being equally potent in affecting cell viability (Fig. 1A). The toxicity predictions of both dasatinib and imatinib from the NET assays are consistent with the clinical cardiotoxic reports for these compounds (Supplemental Table S1).

Furthermore, the assay outcomes of the EGF receptor inhibitors, erlotinib and lapatinib, are also consistent with clinical observations. In patients, erlotinib rarely causes adverse cardiac events, while lapatinib is associated with LVD and cardiomyopathy (Supplemental Table S1). In the NET assays, erlotinib had little effect. It only caused a low degree of oxidative stress at ≥25 μM and a low level of energy metabolism disruption at 100 μM (Fig. 1A). In contrast, lapatinib started to cause death of hPSC-CMs at 13 μM, likely due to a combination of mitochondrial membrane depolarization, energy depletion, oxidative stress, and apoptosis.

The strength of the NET assays for profiling different mechanisms leading to drug-induced cardiotoxicity is further illustrated by SMKIs that inhibit non-growth factor pathways (Fig. 1B and C). Perifosine, XL765, temsirolimus, and everolimus are SMKIs that inhibit the PI3K/AKT/mTOR pathway. Perifosine targets AKT, whereas XL765 inhibits both PI3K and mTOR (Gills and Dennis, 2009; Zhao et al., 2019). Results from the NET assays indicate that perifosine is more toxic to hPSC-CMs than XL765 and each has a unique mechanistic toxicity profile. Perifosine primarily induced apoptosis and energy metabolism disruption. In contrast, XL765 did not induce apoptosis at any tested concentration, but it did result in low to moderate levels of oxidative stress, mitochondrial toxicity, and energy disruption (Fig. 1B). Although severe cardiac toxicity has not been reported to date, clinical trials for both drugs are still in progress.

Both mTOR inhibitors, temsirolimus and everolimus, demonstrated cardiac cytotoxicity in most or all the NET assays (Fig. 1B). The one mechanistic difference was that everolimus induced very little oxidative stress compared to temsirolimus. On a molar basis, everolimus and temsirolimus both are very toxic to hPSC-CMs and are potent disruptors of energy metabolism (Fig. 1B). This is consistent with the known biological activity of mTOR in regulating energy and metabolic activity (Saxton and Sabatini, 2017). Although both temsirolimus and everolimus have been approved by the FDA for cancer therapy, there have been reports of various drug-related clinical cardiac adverse events (Supplemental Table S1).

Tozasertib (pan-aurora kinase inhibitor), barasertib (Aurora B inhibitor), and alvocidib (CDK inhibitor) are all cell cycle regulators. Among these three SMKIs, alvocidib is the most cardiotoxic on a molar basis in the NET assays (Fig. 1C). Although these three inhibitors showed different mechanistic profiles in the NET assays, mitochondrial toxicity did not appear to be a major mechanism for any of these drugs. The NET assays not only revealed that these three cell cycle inhibitors demonstrate different degrees of cardiotoxicity, but they also point to different potential mechanisms of cardiotoxicity. The fact that clinical development of tozasertib has been terminated due to severe cardiac liabilities is consistent with the prediction of cardiotoxicity by these NET assays. In addition, although barasertib and alvocidib are currently still in clinical trials, some adverse cardiac events have been reported (Supplemental Table S1).

Selumetinib and PD325901 were selected as examples of MEK inhibitors. PD325901 has no reports of serious adverse clinical cardiac events, while selumetinib has induced cardiomyopathy in some patients. However, the NET assays showed both SMKIs to be safe in hPSC-CMs, which makes selumetinib a false negative in the NET assays (Fig. 1C).

3.2. Categorical analysis of NET in hPSC-CMs

Beyond the conclusions drawn above, it is important to correlate these in vitro drug responses to clinically relevant drug dosages, as this would be valuable for translating in vitro results into clinical predictions. This classification of drug-induced cardiac cytotoxicity levels in hPSC-CMs relevant to clinical C_{max} concentrations for all drugs in all NET assays is shown in a heatmap format in Fig. 2. These data are based on the conversion of EC_{50} or IC_{50} values from dose response assays (see Supplement Table S2–6) into FoldC_{max} values (see Supplement Table S1 for clinical C_{max} values).

This analysis revealed that overall cell viability is a good predictor of non-electrophysiological cardiotoxicity. Compounds were grouped into four cardiotoxicity "NET Categories" based on the FoldC_{max} drug concentrations that affected cell viability (Fig. 2). Category 1 would be predicted to be safe compounds (axitinib, erlotinib, selumetinib, and PD325901), while Category 2 would be predicted to have low risk (everolimus). Category 3 would be predicted to have intermediate risk (barasertib, dasatinib, sunitinib, XL765, and tozasertib), and Category 4 would be drugs predicted to have the highest risk for non-electrophysiological toxicity (lapatinib, temsirolimus, imatinib, sorafenib, lestaurtinib, perifosine, and alvocidib). Drugs whose assay

Kinase Inhibitor	Cell Viability Assay	Mechanistic Toxicity Assays				NET Category
		Apoptosis	Mitochondrial Depolarization	Oxidative Stress	Energy Depletion	
Axitinib	N	N	N	N	N	1
Erlotinib	N	N	N	N	N	
Selumetinib	N	N	N	N	N	
PD325901	N	N	N	N	N	
Everolimus	767	833	1250	N	538	2
Barasertib	181	493	529	435	202	3
Dasatinib	171	131	N	118	145	
Sunitinib	161	222	133	127	172	
XL765	120	N	0.05	60	N	
Tozasertib	41	38	124	105	84	
Lapatinib	17	N	22	28	25	4
Temsirolimus	8.2	12.3	7.4	7.5	7.0	
Imatinib	6.5	N	N	13	9.2	
Sorafenib	1.5	N	0.2	N	1.8	
Lestaurtinib	0.6	1.1	1.0	1.3	1.6	
Perifosine	0.7	1.5	2.0	2.1	1.4	
Alvocidib	0.03	0.19	N	0.19	0.04	

IC_{50} or EC_{50}
non-measurable (N)
>300 FoldC_{max}
30-300 FoldC_{max}
<30 FoldC_{max}

Fig. 2. Assessment of In Vitro Non-Electrophysiological Cardiac Toxicity of SMKIs at Clinically Relevant Concentrations (FoldC_{max}).
In vitro IC_{50} or EC_{50} values calculated from dose response curves (Supplemental Fig. S2-S6) for each drug were converted to FoldC_{max} for each assay (see Supplemental Table S1 for references for C_{max} values). Drug toxicities were then classified into quartile levels from low to high based on FoldC_{max}: Level 1) not measurable; 2) >300 FoldC_{max}; 3) 30–300 FoldC_{max}; and 4) <30 FoldC_{max}. The last column shows the overall predicted clinical cardiac risk as NET Categories: 1) no risk; 2) low risk; 3) intermediate risk; and 4) high risk.

results were relatively close to the cutoff boundaries could reasonably be argued to fall into either category. However, classification was kept consistent across compounds and was based on cell viability. We will discuss the concordance of these classifications with clinical outcomes in the Discussion (Fig. 8).

3.3. SMKI-induced electrophysiological effects in hPSC-CMs

Although SMKIs mainly cause direct cardiotoxicity, many of them are also proarrhythmogenic. For example, sunitinib and dasatinib are associated with clinical QT prolongation and TdP. Although arrhythmia differs from direct cell damage or death, significant heart tissue damage can potentially lead to arrhythmia (Aon et al., 2009; Reimer and Ideker, 1987). To build a more complete view of SMKI-induced CM toxicity, the electrophysiological effects of nilotinib, which is a prominent SMKI with a black box warning of cardiotoxicity, plus the previous 17 SMKIs, were analyzed in MEA assays.

MEA analyses were used to determine FPDc, spike amplitudes, and arrhythmic waveforms of hPSC-CMs following drug treatment. The percentage effects of all three parameters were presented in a heatmap format (Fig. 3). SMKI-induced iAEs were divided into four levels. Dasatinib started to induce Level-3 iAEs at 30 μM and Level-4 at 72 μM. Sunitinib induced Level-4 iAEs at 8.7 μM and 30 μM (two wells had iAEs; one well was quiescent), and all wells were quiescent at 72 μg. Nilotinib had the most severe electrophysiological effects, inducing Level-4 iAEs at all tested drug concentrations. Barasertib only induced Level-2 iAEs at 30 μM, and all wells were quiescent at 72 μM. Three drugs (lestaurtinib, sorafenib, and alvocidib) induced quiescence at either 30 or 72 μM without detectable arrhythmic events.

SMKI-induced FPDc effects classified into six levels were plotted in a heatmap format for an easy comparison (Fig. 3). Instead of prolongation, three compounds (temsirolimus, lestaurtinib, and PD325901) showed more than 15% reduction in FPDc at various concentrations. Six SMKIs (axitinib, erlotinib, lapatinib, perifosine, XL765, and selumetinib) showed insignificant FPDc changes (±15%) at all concentrations. Meanwhile, seven SMKIs (dasatinib, sunitinib, nilotinib, alvocidib, barasertib, and tozasertib) showed greater than 15% FPDc prolongation at various concentrations. In contrast, many drugs (sunitinib, lestaurtinib, sorafenib, alvocidib, and barasertib) completely stopped electrical activity in hPSC-CMs at higher concentrations and were recorded as quiescent (Q). Other drugs, such as alvocidib and everolimus, resulted in beats below threshold (BBT) at higher concentrations. FPDc was not measurable for either Q or BBT wells.

Spike amplitude in MEA studies is analogous to the sodium-spike "R" peak in electrocardiogram (ECG) traces (Nerbonne and Kass, 2005). Dose responses of SMKIs causing SAS in the MEA assays (Supplemental Fig. S7) were used to classify five levels of SAS in a heatmap format (Fig. 3). Axitinib, erlotinib, and PD325901 showed baseline levels of SAS that were less than 25% at all tested concentrations, whereas lapatinib and XL765 had modest SAS effects that were less than 50% only at the highest concentration tested. Imatinib, dasatinib, perifosine, temsirolimus, and selumetinib induced low to medium SAS, with 25–50%

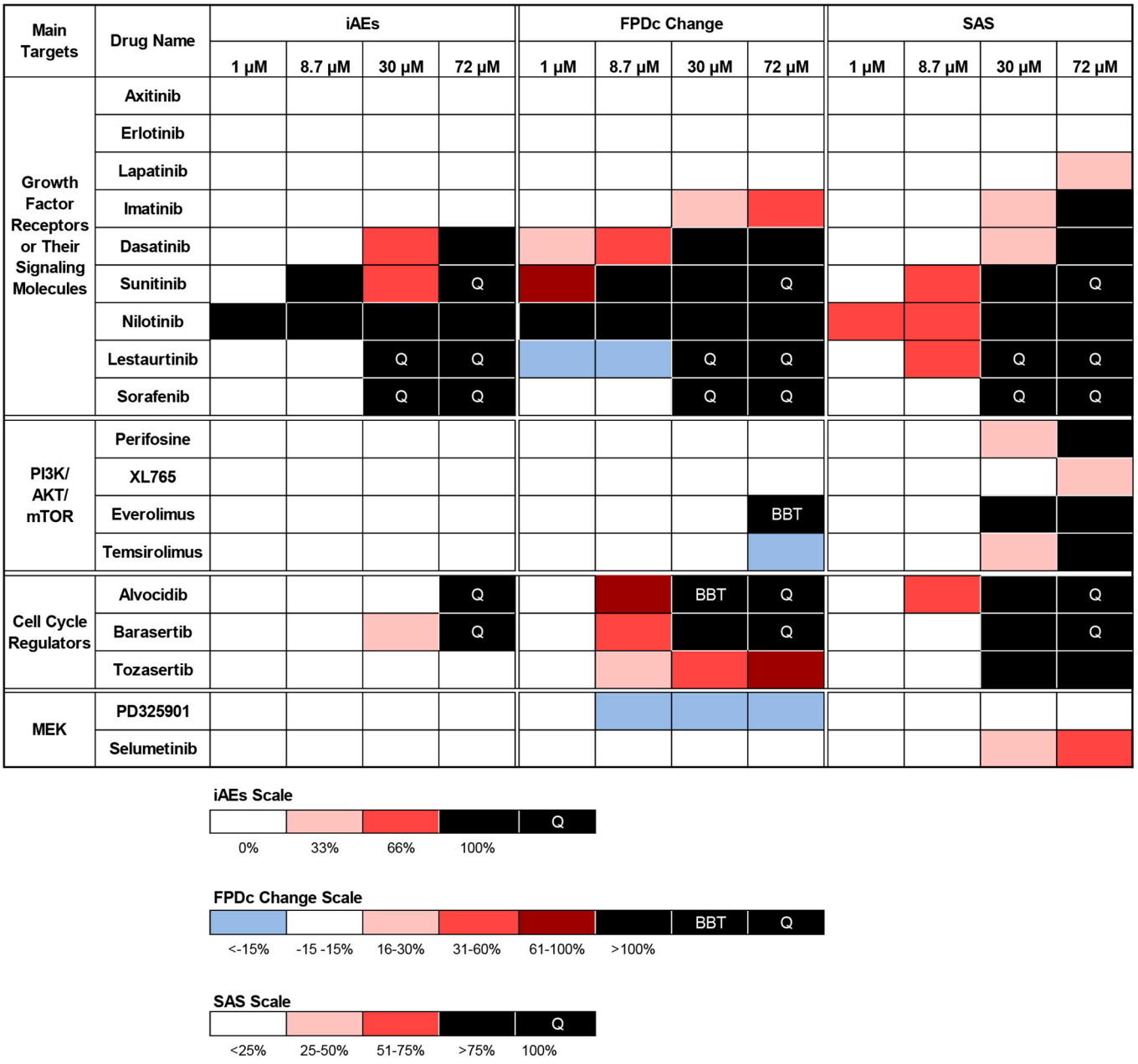

Fig. 3. Electrophysiological Effects of SMKIs on hPSC-CMs.
The electrophysiological effects of SMKIs on hPSC-CMs were measured using an Axion MEA system. The percentage change of three parameters, drug-induced in vitro arrhythmic events (iAEs), corrected field potential duration (FPDc), and spike amplitude suppression (SAS), were plotted in a heatmap format based on the average drug effects of triplicate wells at each concentration. When waveforms were not detectable after drug treatment, the well was labeled quiescent (Q). For quiescent wells, iAEs and FPD were not measurable, and SAS was recorded as 100%. FPD was also not measurable when beats were below the threshold (BBT) of 300 μV.

suppression at 30 μM and 50–100% at 72 μM. Barasertib, tozasertib, everolimus, and sorafenib induced a higher degree of SAS, with greater than 75% suppression at 30 μM. And nilotinib, sunitinib, alvocidib, and lestaurtinib showed the most severe SAS, with greater than 50% suppression at 1–8.7 μM. Taken together, these SMKIs showed unique MEA profiles with different types and degrees of electrophysiological alterations in hPSC-CMs.

3.4. *Categorical analysis of electrophysiological effects of SMKIs in hPSC-CMs*

To get a more clinically relevant understanding, drug concentrations presented in Fig. 3 were converted to FoldC_{max} for each drug, as was done in the NET assay analyses. The arrhythmogenesis of SMKIs was classified based on the FoldC_{max} value that corresponded to iAE_{33} (Fig. 4A). Out of 18 SMKIs studied, 14 had no iAEs and were grouped into Category-1. Dose response curves of the four SMKIs that induced iAEs are plotted in Fig. 4B. Barasertib was in Category-2, as it induced iAEs only in one of three wells (33%) at 30 μM (177 FoldC_{max}), and all three wells were quiescent at 72 μM. Dasatinib and sunitinib were in Category-3. Sunitinib induced 100% iAEs at 48 FoldC_{max} (all three wells), at 167 FoldC_{max} (two wells; one well was quiescent), and all wells were quiescent at 400 FoldC_{max}. Examples of in vitro arrhythmic waveforms induced by sunitinib in hPSC-CMs are shown in Fig. 4C. Dasatinib showed iAE effects in 66% of wells at 143 FoldC_{max} and 100% at 343 FoldC_{max}. Nilotinib, on the other hand, showed 100% iAE effect

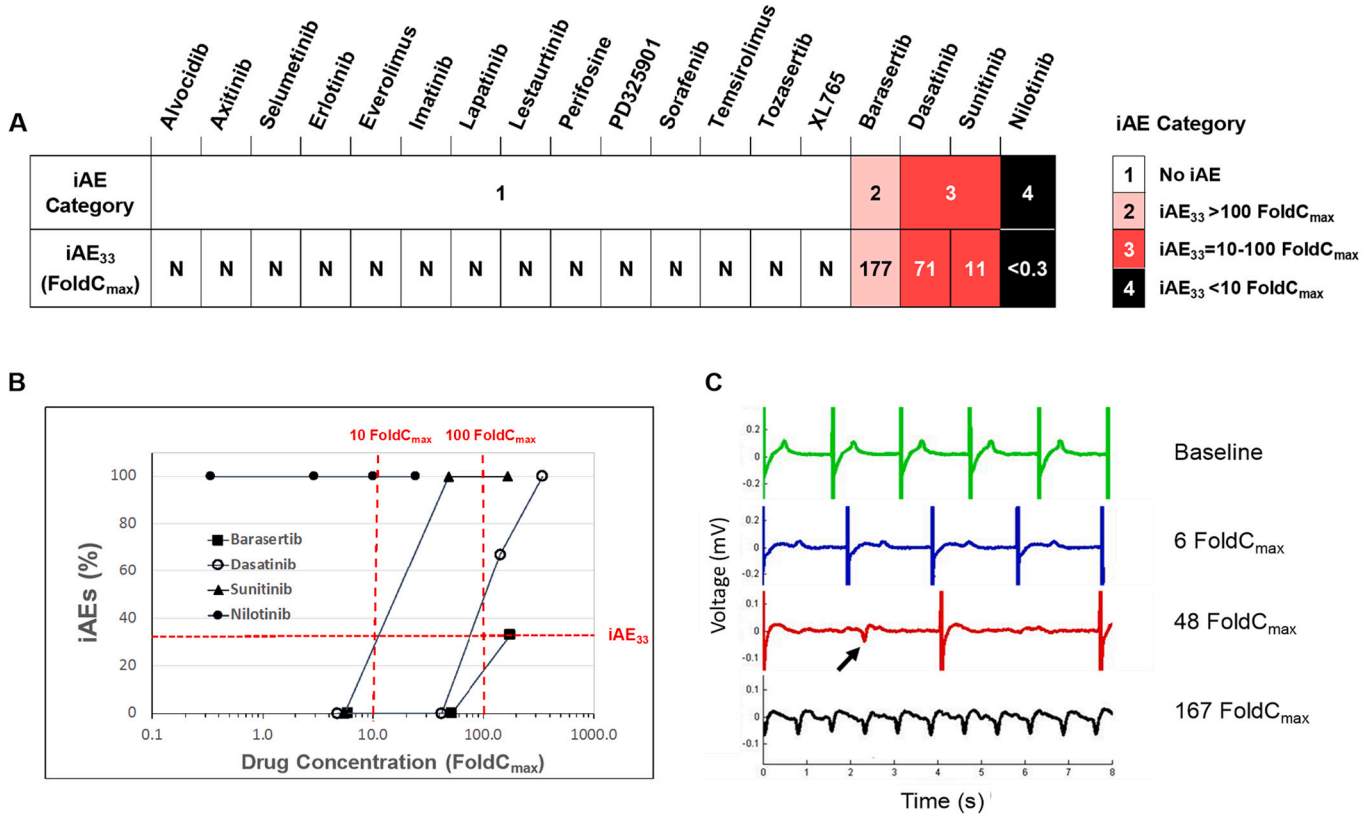

Fig. 4. SMKI-induced Arrhythmogenesis in hPSC-CMs at Clinically Relevant Drug Concentrations ($FoldC_{max}$).
A) SMKIs were categorized based on iAE_{33} estimated values (see panel B) in MEA assays using hPSC-CMs: 1) no iAEs observed (designated as "N"); 2) $iAE_{33} > 100$ $FoldC_{max}$; 3) iAE_{33} 10–100 $FoldC_{max}$; and 4) $iAE_{33} < 10$ $FoldC_{max}$. **B)** iAE dose response plots, in $FoldC_{max}$ units, of Category 2–4 SMKIs are shown. These were used for iAE_{33} estimation, as marked by the horizontal dashed line. The vertical dashed lines (10 and 100 $FoldC_{max}$) are the category boundaries. **C)** MEA traces of sunitinib-treated hPSC-CMs with the arrow highlighting a typical drug-induced arrhythmic waveform at 48 $FoldC_{max}$. At 167 $FoldC_{max}$ a fibrillation state was induced.

at all four testing concentrations, starting at less than 0.3 $FoldC_{max}$, which made it a Category-4 drug. The classification of nilotinib in the high-risk category is consistent with the black box warning of cardiac toxicity for nilotinib.

Dose-dependent FPDc prolongation (FPDcP) is a widely used measurement of drug-induced electrophysiological effects both in vitro and clinically. To evaluate the FPDc effects of SMKIs in hPSC-CMs in a clinically relevant context, the percent change in FPDc measured in the MEA assays was plotted against $FoldC_{max}$ (Fig. 5B and C). Classification of FPDc change was summarized in a heatmap format (Fig. 5A). Category-1 drugs (lestaurtinib, PD325901, and temsirolimus) showed a reduction of FPDc. Category-2 drugs (sorafenib, perifosine, erlotinib, selumetinib, lapatinib, XL765, everolimus, and axitinib) showed insignificant effect at any concentration, defined as ±15% FPDc alteration. Among 18 SMKIs, none of them was in Category-3, which is defined as mild effects with $FPDcP_{30} > 50$ $FoldC_{max}$. Category-4 drugs (barasertib, tozasertib, dasatinib, and imatinib) demonstrated moderate effects, $FPDcP_{30}$ between 5 and 50 $FoldC_{max}$. Finally, Category-5 drugs (sunitinib, alvocidib, and nilotinib) showed severe effects ($FPDcP_{30} < 5$ $FoldC_{max}$). The correlation of the iAE and FPDc results to the clinical cardiac liabilities will be described in the Discussion (Fig. 7).

In vitro drug effects on SAS measurement in the MEA assays have been rarely investigated, but one study concluded that it added little additional predictive value for TdP risk prediction (Blinova et al., 2018). To test this conclusion, SAS was analyzed in the same fashion as the FPDc measurements. The percent changes in SAS of SMKIs were plotted against $FoldC_{max}$ (Fig. 6B). SMKIs were categorized based on $FoldC_{max}$ values of SAS_{30} and summarized in a heatmap format (Fig. 6A). Category-1 drugs (axitinib, erlotinib, PD325901) showed no SAS effects. Category-2 drugs (everolimus and dasatinib) had minimal SAS effects, $SAS_{30} > 100$ $FoldC_{max}$. Category-3 drugs (barasertib, XL765, tozasertib, lapatinib, sunitinib, and selumetinib) demonstrated moderate SAS effects, SAS_{30} = 10–100 $FoldC_{max}$. Category-4 drugs (imatinib, temsirolimus, sorafenib, alvocidib, perifosine, lestaurtinib, and nilotinib) demonstrated severe SAS effects, SAS30 < 10 $FoldC_{max}$. The predictive relevance of SAS classification will be addressed below (Fig. 8) in the Discussion.

4. Discussion

Cardiac liabilities of many SMKIs used in cancer therapy often go undetected in FDA-recommended in vitro hERG assays and in vivo animal safety studies during preclinical drug development. This is evidenced by the many cardiac adverse events observed in patients treated with SMKIs (Supplemental Table S1). Most of these clinical cardiac adverse events have been associated with inhibition of kinase-dependent pathways that are involved with non-electrophysiological cardiac effects such as cardiomyopathy, HF, and LVD (Laverty et al., 2011). Contrary to well-established approaches to assess electrophysiologically-related safety effects during development, there are no FDA-recommended in vitro assays for predicting cardiac structural damage, metabolic health, or direct cardiotoxicity. Some groups have approached this important problem with primarily image-based assays (Clements et al., 2015; Guo et al., 2013; Lamore et al., 2017; Pointon et al., 2013; Sharma et al., 2017; Thomas, 2012). We sought to extend these efforts by developing and optimizing a panel of microplate-based fluorescent or luminescent

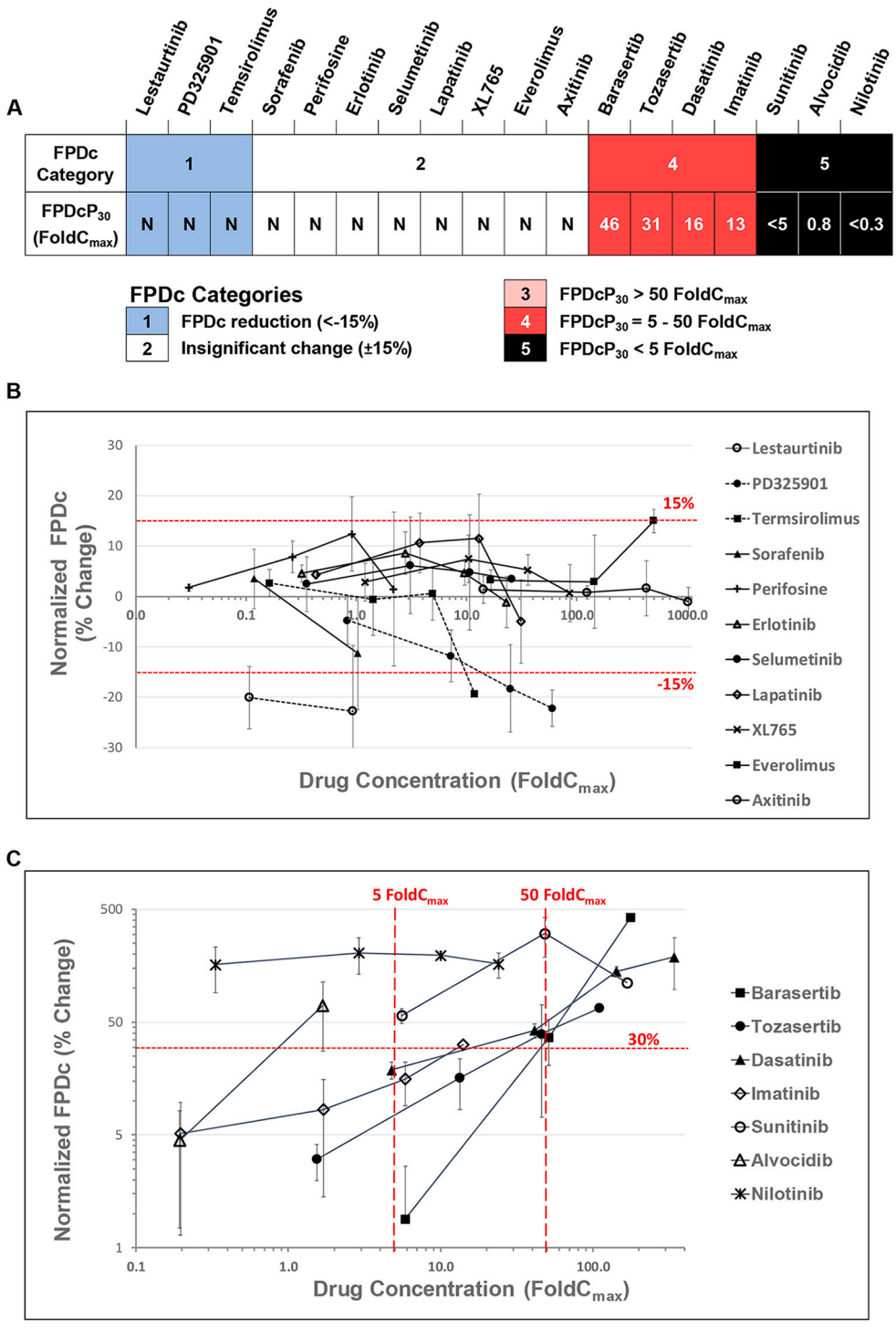

Fig. 5. SMKI-induced FPDc Effects on hPSC-CMs at Clinically Relevant Concentrations ($FoldC_{max}$).
A) FPDc dose response curves (panels B and C) were used for estimating $FPDcP_{30}$ values to define five FPDc Categories: 1) SMKIs that reduced FPDc more than 15% at least at one concentration; 2) SMKIs with insignificant FPDc change (±15%); 3) SMKIs that prolonged FPDc by 30% ($FPDcP_{30}$) at >50 $FoldC_{max}$; 4) SMKIs with $FPDcP_{30}$ between 5 and 50 $FoldC_{max}$; and 5) SMKIs with $FPDcP_{30}$ < 5 $FoldC_{max}$. None of the testing SMKIs fell in the Category-3. The $FPDcP_{30}$ values for FPDc Categories 1 and 2 could not be calculated and, therefore, were listed as non-significant (N). **B)** FPDc dose response plots of SMKIs in FPDc Categories 1 and 2. Values between the dashed lines (±15%) were considered insignificant changes of FPDc. Three SMKIs (dashed lines) showed FPDc reduction greater than 15% at least at one concentration. **C)** FPDc dose response plots of SMKIs in FPDc Categories 4–5. The horizontal dashed line marks $FPDcP_{30}$. The vertical dashed lines mark the classification boundaries (5 and 50 $FoldC_{max}$) for this group.

hPSC-CM assays that enhance predictiveness and examine underlying functional mechanisms involved in non-electrophysiological toxicities (NET).

The NET assays described herein are less dependent on expensive instrumentation, and importantly, they are also more sensitive at earlier time points when compared to some image-based assays (Clements et al., 2015; Pointon et al., 2013). We were able to detect apoptosis, oxidative stress, and mitochondrial membrane depolarization after 18 h drug exposure. However, Pointon's study necessitated 72 h drug treatment to detect toxicity in mitochondria, as morphological damage in hESC-CMs was still undetectable by 24 h. A possible explanation is that fluorescent imaging tools are less sensitive. A similar study designed to measure structural toxicity using high-content image analysis assays has been published (Clements et al., 2015). Since these assays are more sensitive than the standard fluorescent image analysis used by Pointon's group, they were able to measure drug-induced damage to cell membranes and mitochondrial membranes, as well as Ca + mobilization, after 24 h drug treatment. However, only two SMKIs, axitinib and sunitinib, were included among the 13 validation compounds in this study (Clements et al., 2015).

Another group employed a simple non-image-based viability assay, which is similar to one of our NET assays, for assessing tyrosine kinase

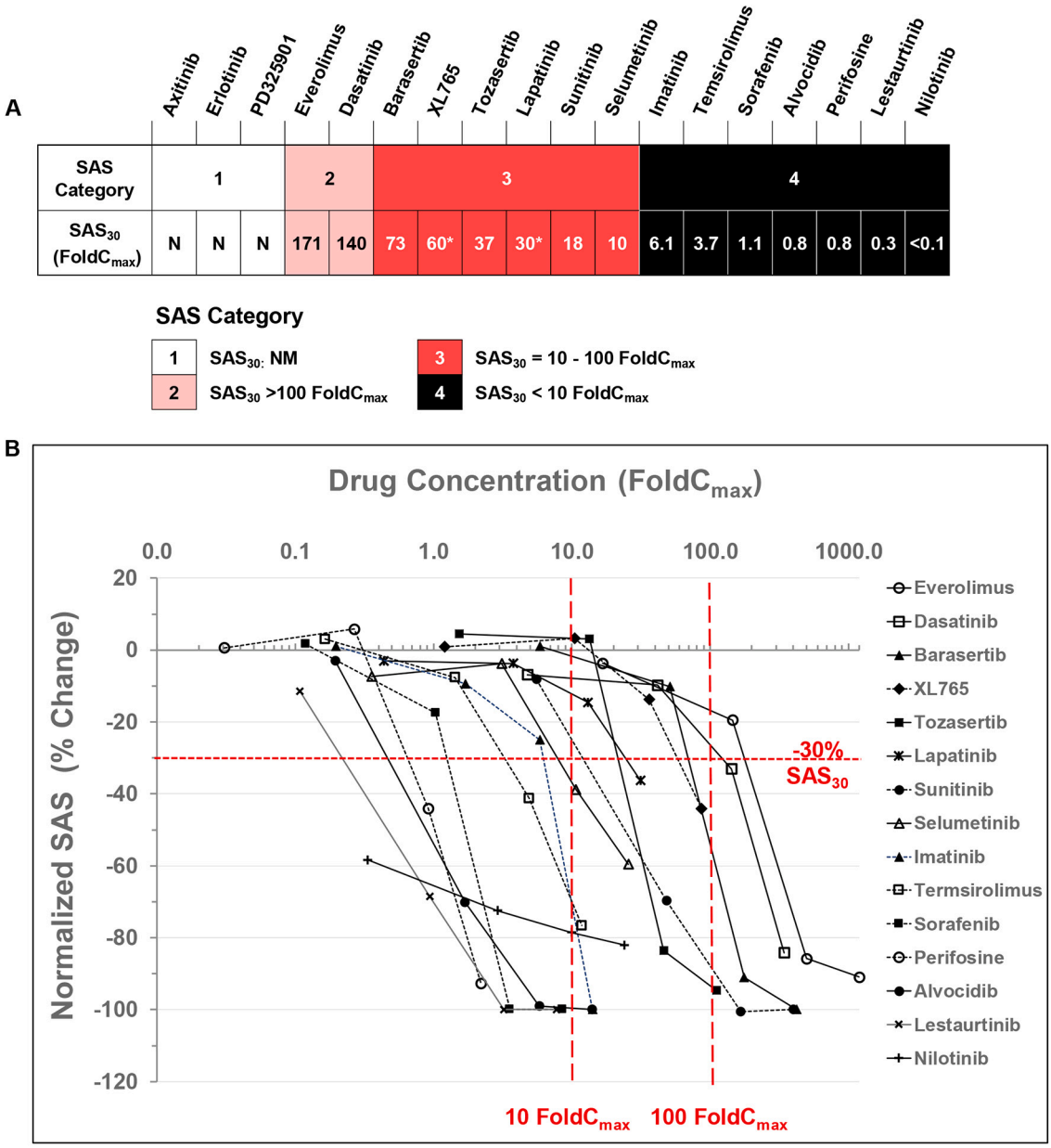

Fig. 6. SMKI-induced SAS in hPSC-CMs at Clinically Relevant Concentrations ($FoldC_{max}$).
A) Based on the $FoldC_{max}$ that induced 30% SAS (SAS_{30}), SMKIs were grouped into four SAS Categories: 1) non-measurable SAS_{30} values (designated as "N"); 2) SAS_{30} > 100 $FoldC_{max}$; 3) SAS_{30} between 10 and 100 $FoldC_{max}$; and 4) SAS_{30} < 10 $FoldC_{max}$. **B)** For SMKIs in SAS Categories 2–5, average SAS effects of triplicate wells at each concentration were plotted versus $FoldC_{max}$. Where possible, GraphPad was used to calculate SAS_{30} from the dose response curves, otherwise, extrapolations were made from Excel, such as XL765 and lapatinib, which are indicated with an "*". The horizontal dashed line marks SAS_{30}. The vertical dashed lines mark the classification boundaries (10 and 100 $FoldC_{max}$).

inhibitor (TKI)-induced cardiac toxicity in hPSC-CMs (Sharma et al., 2017). In this study, cytotoxicity and cell contractility assessments were combined for establishing a "TKI cardiac safety index," which could be helpful to gauge the overall cardiotoxicity of TKIs. However, these assays are neither capable of distinguishing between electrophysiological and non-electrophysiological cardiac toxicity, nor provide mechanistic information. Importantly, our study goes beyond these studies by combining NET assays with MEA assays, which enables the assessment of both electrophysiological and non-electrophysiological cardiac toxicities. Furthermore, the NET assays also provide insight into important mechanistic toxicity pathways, including apoptosis, mitochondrial depolarization, oxidative stress, and energy depletion.

To provide more clinically relevant analyses, the drug concentrations of the NET data were converted to $FoldC_{max}$ values, and categorical analytical methods were used for toxicity rankings. The predictive value of these analytical approaches was tested with 17 compounds in the NET assays and 18 compounds in the electrophysiological assays that covered several different SMKI categories and pathways. This dual-armed approach involving both electrophysiological and non-electrophysiological focused assays provided a more holistic prediction of SMKI-induced cardiac toxicities with excellent concordance with clinical experience (see below). In addition, this approach also provided valuable mechanistic insight into drug-specific cardiac toxicities.

4.1. Correlation of toxicity classifications with clinical experience

It is widely believed that in vitro FPDc is a correlate of clinical QT measurements and that iAEs detected in hPSC-CM cultures are a potential correlate of clinical arrhythmia. In Fig. 7, the categorical results for each drug from the FPDc Assay (Fig. 5) are paired with reported clinical QTc observations (Supplemental Table S1), and the categorical results from the iAE Assay (Fig. 4) are paired with reported clinical arrhythmia observations (Supplemental Table S1). The concordance columns list "true positive (TP)" or "true negative (TN)" if the in vitro predictions are concordant between the pairs of in vitro assay predictions and clinical experience (Fig. 7). Non-concordance is indicated as either a "false negative (FN)" if the in vitro assays incorrectly predicted the compound would be relatively safe, or a "false positive (FP)," if the in vitro assays incorrectly predicted the compound would be relatively toxic. There is striking concordance between the FPDc Assay

Kinase Inhibitor	FDA Status	Clinical QTc Prolongation	FPDc Assay	FPDc Concordance	Clinical Arrhythmia	iAE Assay	iAE Concordance
PD325901	Phase 2	not reported	N	TN	not reported	N	TN
Lestaurtinib	Phase 2/3	not reported	N	TN	not reported	N	TN
Temsirolimus	approved	not reported	N	TN	not reported	N	TN
Axitinib	approved	not reported	N	TN	not reported	N	TN
Selumetinib	approved	not reported	N	TN	not reported	N	TN
Erlotinib	approved	not reported	N	TN	not reported	N	TN
Everolimus	approved	not reported	N	TN	not reported	N	TN
Perifosine	Phase 2/3	not reported	N	TN	not reported	N	TN
XL765	Phase 2	not reported	N	TN	not reported	N	TN
Sorafenib	approved	QTc prolongation (rare)	N	FN	possible risk of TdP	N	FN
Lapatinib	approved	QTc prolongation	N	FN	possible risk of TdP	N	FN
Barasertib	Phase 1/2	not reported	46	FP	not reported	177	FP
Tozasertib	Phase 2 terminated	QTc prolongation	31	TP	not reported	N	TN
Dasatinib	approved	QTc prolongation	16	TP	possible risk of TdP	71	TP
Imatinib	approved	QTc prolongation	13	TP	not reported	N	TN
Sunitinib	approved	QTc prolongation	<5	TP	possible risk of TdP	11	TP
Alvocidib	Phase 2 completed	QTc prolongation	1	TP	not reported	N	TN
Nilotinib	approved	QTc prolongation	<0.3	TP	risk of TdP, sudden death (black-box warning)	<0.3	TP

Fig. 7. Concordance of FPDc and iAE results with Clinical Electrophysiological Cardiac Liability.
Using a heatmap format, we compared the predictivity of FPDc and iAE Categorical Analyses of the in vitro hPSC-CM assays to reported clinical electrophysiological cardiac liabilities for each SMKI. The FPDc and iAE Assay columns list $FoldC_{max}$ for each drug and are shaded the same as in Fig. 4A and 5A. N = no significant effect. The Clinical QTc Prolongation column is shaded with the lightest shade for no reported prolongation, the medium shade for rare prolongation, and the darkest shade for frequent prolongation. The Clinical Arrhythmia column is also shaded with the lightest shade for no reported TdP or arrhythmia, medium shade for possible risk of TdP, and black for TdP risk with a black-box warning. The assay concordance of the paired FPDc/Clinical QT and iAE Assay/Clinical Arrhythmia outcomes are listed for each assay. When an in vitro prediction is concordant with clinical experience, it is recorded as a "TP" ("true positive") for a drug associated with cardiac toxicity in patients, or a "TN" ("true negative") for a drug with little to no reported clinical adverse events. When an in vitro prediction is discordant with clinical observations, it is indicated as either a "FP" ("false positive") for a clinically safe drug, or "FN" ("false negative") for a drug with clinical adverse effects.

and clinical QTc. All six compounds (tozasertib, dasatinib, imatinib, sunitinib, alvocidib, and nilotinib), which were categorized in the top two most toxic categories in the FPDc Assay, induce significant clinical QTc prolongation. Additionally, three SMKIs (nilotinib, sunitinib, and dasatinib) have demonstrated clinical risks of TdP and/or sudden death "black box warnings," and clinical trials of tozasertib were terminated due to serious adverse cardiac events (Green et al., 2011) (Fig. 7). These studies also suggest that in this set of compounds there is little toxicity

Kinase Inhibitor	FDA Status	Clinical Cardiac Adverse Events (non-Ephys)	Viability Assay	Viability Concordance	SAS Assay	SAS Concordance
Axitinib	approved	HF (rare)	N	TN	N	TN
Erlotinib	approved	HF (rare)	N	TN	N	TN
PD325901	Phase 2	not reported	N	TN	N	TN
Selumetinib	approved	cardiomyopathy	N	FN	10	TP
Everolimus	approved	chest pain, hypertension, HF (rare)	767	TP	171	TP
Barasertib	Phase 1/2	chest pain, hypertension, myocardial ischaemia	181	TP	73	TP
Dasatinib	approved	HF, cardiomyopathy, LVD	171	TP	140	TP
Sunitinib	approved	HF, cardiomyopathy, LVD	161	TP	18	TP
XL765	Phase 2	not reported	120	FP	60*	FP
Tozasertib	Phase 2 terminated	HF	41	TP	37	TP
Lapatinib	approved	LVD, cardiomyopathy	17	TP	30*	TP
Temsirolimus	approved	chest pain, hypertension	8.2	TP	3.7	TP
Imatinib	approved	HF, cardiomyopathy, LVD	6.5	TP	6.1	TP
Sorafenib	approved	HF, MI	1.5	TP	1.1	TP
Lestaurtinib	Phase 2/3	LVD	0.6	TP	0.3	TP
Perifosine	Phase 2/3	not reported	0.7	FP	0.8	FP
Alvocidib	Phase 2 completed	not reported	0.03	FP	0.8	FP
Nilotinib	approved	HF, cardiomyopathy, ischemic heart disease	N/A	N/A	<0.1	TP

Fig. 8. Concordance of Viability and SAS Assays with Clinical Non-Electrophysiological Cardiac Liability.
A heatmap is used to compare the results from the in vitro Viability and SAS assays to clinically reported non-electrophysiological cardiac adverse events for each SMKI. The Viability Assay and SAS Assay columns list the FoldC_{max} for each drug and are shaded the same as in Fig. 2 and 6A. N = no significant effect. Clinical Cardiac Adverse Events are subjectively shaded with a lighter shade for no or rarely reported events, a medium shade for less frequent or less severe events, and the darkest shade for more frequent and severe events based on FDA prescribing info and other publications (Supplemental Table 1). The concordance of the Viability or SAS assays with the clinical observations are recorded separately. When an in vitro prediction is concordant with clinical experience, it is recorded as a "TP" ("true positive") for a drug associated with cardiac toxicity in patients, or a "TN" ("true negative") for a drug with little to no reported clinical adverse events. When an in vitro prediction is discordant with clinical observations, it is indicated as either a "FP" ("false positive") for a drug with little to no reported clinical adverse events, or "FN" ("false negative") for a drug with reported clinical adverse effects.

concern with compounds that shorten FPDc. Out of the 18 SMKIs analyzed, there are only two "false negatives" (sorafenib and lapatinib) and one potential "false positive" (barasertib) (Fig. 7). It is clear from these results that the electrophysiological MEA assays misidentify sorafenib and lapatinib as safe compounds, however, the NET assays (Fig. 2) predict that these two compounds are toxic, with a mechanism likely related to mitochondrial depolarization. These results further highlight the advantage of combining electrophysiological and non-electrophysiological assays to improve predictiveness for potential drug-induced clinical cardiotoxicities.

The concordance analysis of the Viability Assay with clinical non-electrophysiological adverse events resulted in three potential false positives (XL765, perifosine, and alvocidib) (Fig. 8). Interestingly, all these compounds are currently in clinical trials and have not yet been approved by the FDA. It would be important to continue to monitor their clinical adverse events as more patients are exposed over longer periods to determine whether cardiac toxicities are associated with these drugs in the clinic. Fig. 8 also highlights the value of using FoldC_{max} for assessing drug-induced cardiotoxicity. For example, the EC_{50} of everolimus and sunitinib in the Viability Assay are 46 μM and 29 μM, which does not separate these two SMKIs well (Supplemental Fig. S2). However, when FoldC_{max} is used, the EC_{50} of everolimus is converted to 767 FoldC_{max}, which makes it a Category 2 compound (minimal toxicity), but the EC_{50} of sunitinib is 161 FoldC_{max}, which makes it a Category 3 compound (moderate toxicity). It has been reported that everolimus only causes indirect adverse cardiac events in patients with pre-existing conditions (Karvelas et al., 2018), while adverse cardiac events were reported in a high percentage of patients taking sunitinib (Khakoo et al., 2008). These results suggest that, when possible, normalization to C_{max} is more predictive for drug-related cardiac liabilities than absolute drug concentrations. This does raise a problem for preclinical drug candidates without C_{max} data. However, in these cases, animal data could be used to estimate human C_{max} ranges.

The SAS Assay is one of three MEA-based assays we used to measure electrophysiological alterations in CMs, but unlike the FPDc Assay and iAE Assay, to date it has not been shown to have significant predictive value for TdP-risk prediction (Blinova et al., 2018). When comparing these three assay results, we found 15 out of 18 SMKIs showed SAS effects, seven SMKIs prolonged FPDc, and four SMKIs induced iAEs (Fig. 3). These data suggest that SMKIs that induce iAEs also prolong FPDc and have SAS effects. However, eight out of the 15 SMKIs that show SAS effects do not prolong FPDc or induce iAEs. When we further compared the SAS Categorical Analysis to reported clinical electrophysiological cardiac liabilities for each SMKI (Supplemental Fig. S8), the concordance of the paired SAS/Clinical QT Prolongation and SAS/Clinical Arrhythmia were 61% and 44%, respectively. This suggests the SAS Assay is not a reliable assay for predicting clinical QT prolongation or arrhythmia (e.g., TdP risk).

However, we found there was a strong correlation between the SAS Assay and the Viability Assay (Fig. 8), even though the SAS Assay measures electrophysiological activities in CMs, while the Viability Assay measures general health of CMs. It has been shown most drugs that caused damage or death of hPSC-CMs had severe SAS effects in our studies. Out of the 17 SMKIs tested, selumetinib was the only compound that was strongly discordant between the Viability Assay and SAS Assay. Interestingly, selumetinib, which is associated with cardiomyopathy, was only identified as a cardiotoxic compound in the SAS Assay and not in the other assays. Comparing these two in vitro assay results with non-electrophysiological cardiac adverse events in patients, such as HF, LVD, and cardiomyopathy (Fig. 8), 13 drugs were found to be concordant, three drugs (XL765, perifosine, and alvocidib) were potential false positives, and one (selumetinib) was "mixed," meaning the Viability Assay was discordant but the SAS Assay was concordant with clinical reports. Taken together, this suggests that the SAS Assay may have potential as a supporting tool for evaluation of non-electrophysiological cardiotoxicity, however, more data will be needed to support this.

Table 1 presents the specificity, sensitivity, and accuracy calculations of these predictive models for all the electrophysiological and non-electrophysiological assays. These calculations were carried out on all tested SMKIs, however, since some of these drugs are still in clinical development and do not have extensive clinical history, the same calculations were repeated on the 11 FDA-approved SMKI drugs. When analyzing all versus only FDA approved drugs, both FPDc and iAE Assays had similar predictive characteristics and were better at identifying the safer compounds (90–100% specificity) compared to identifying the toxic drugs (60–75% sensitivity), with an overall accuracy of 82–83% (Table 1). On the other hand, the viability and SAS assays for predicting non-electrophysiological cardiac liability had a slightly different profile. Both Viability and SAS assays showed higher sensitivity for identifying toxic compounds for either all the SMKI compounds (91% and 100%, respectively), and only the FDA-approved SMKIs (88% and 100%, respectively). However, when analyzing all the tested SMKIs, these assays had reduced ability to detect safe compound (50% specificity). This low specificity for all compounds results from three false positives that are still in clinical development, and perhaps more clinical data will help shed light on the accuracy of these predictions. If only FDA-approved SMKIs are considered, both Viability and SAS assays exhibit an overall accuracy, specificity, and sensitivity of 88–100% (Table 1). One of the limitations of this study is that only 18 SMKIs were analyzed, and therefore these predictions may have reduced statistical power when these analyses are expanded to other SMKIs.

This study demonstrates the value of combining in vitro electrophysiological and non-electrophysiological assays for the detection of a wide spectrum of SMKI-induced cardiotoxicities, enabling safety predictions that have strong concordance with clinical experience. In addition to enhanced clinical concordance, the combination of these two classes of assays provides mechanistic insights into drug-induced toxicity. This enhanced predictive power is supported by the fact that the NET assays detected SMKI toxicities missed by electrophysiological assays. In summary, these results support the conclusion that the combination of the electrophysiological and NET hPSC-CM assays have significantly more predictive value than either alone and significantly more than the current FDA-recommended hERG assay. In addition, the

Table 1
Sensitivity, specificity, and accuracy of in vitro assays compared to known clinical cardiac liabilities.

		Predictability for Ephys cardiac liability		Predictability for non-Ephys Cardiac Liability	
		FPDc Assay	iAE Assay	Viability Assay	SAS Assay
All drugs	Accuracy (all concordances)	83%	83%	76%	83%
	Specificity (for negatives)	90%	92%	50%	50%
	Sensitivity (for positives)	75%	60%	91%	100%
Only FDA approved drugs	Accuracy (all concordances)	82%	82%	90%	100%
	Specificity (for negatives)	100%	100%	100%	100%
	Sensitivity (for positives)	67%	60%	88%	100%

The FPDc Assay and iAE Assay were used for predicting electrophysiological cardiac liability including QT prolongation and TdP risk, while the Viability Assay and SAS Assay were used for predicting non-electrophysiological cardiac liability listed in Fig. 8. The sensitivity, specificity, and accuracy of these assays were calculated both for all tested SMKIs and for only FDA approved drugs. Specificity = True Negative / (True Negative + False Positive). Sensitivity = True Positive / (True Positive + False Negative). Accuracy = (True Positive +True Negative) / total number of compounds.

combination of these assays can provide valuable information about potential drug-induced cardiotoxicities early in the drug development process, prior to animal and clinical testing, thus helping to guide the development of safer and more cost-effective compounds.

Funding

Funding for these studies was provided by VistaGen Therapeutics, Inc.

Authors' credit statement

HQX: Conceptualization, Methodology, Investigation, Data Analysis, Writing-Original Draft, Review and Editing, Visualization. CB: Investigation. KB: Writing-Original Draft, Review and Editing, and Visualization. HRS: Data Analysis, Supervision, Writing-Original Draft, Review, Editing, and Visualization.

Disclosures and conflicts of interest

HQX, KB, and HRS are employees of, and stockholders in, VistaGen Therapeutics Inc. but otherwise have no potential conflicts of interest with respect to the research, authorship, or publications of this article.

Declaration of Competing Interest

None.

Acknowledgments

We thank Danajane Katz for providing comments on the figures and editing the supplemental Fig. S1C.

Appendix A. Supplementary data

Supplementary data to this article can be found online at https://doi.org/10.1016/j.taap.2022.115886.

References

Ando, H., Yoshinaga, T., Yamamoto, W., Asakura, K., Uda, T., Taniguchi, T., Ojima, A., Shinkyo, R., Kikuchi, K., Osada, T., et al., 2017. A new paradigm for drug-induced torsadogenic risk assessment using human ips cell-derived cardiomyocytes. J. Pharmacol. Toxicol. Methods 84, 111–127. https://doi.org/10.1016/j.vascn.2016.12.003.

Aon, M.A., Cortassa, S., Akar, F.G., Brown, D.A., Zhou, L., O'Rourke, B., 2009. From mitochondrial dynamics to arrhythmias. Int. J. Biochem. Cell Biol. 41 (10), 1940–1948. https://doi.org/10.1016/j.biocel.2009.02.016.

FDA, 2012. Axitinib full prescribing info insert. https://www.accessdata.fda.gov/drugsatfda_docs/label/2012/202324lbl.pdf.

Blinova, K., Dang, Q., Millard, D., Smith, G., Pierson, J., Guo, L., Brock, M., Lu, H.R., Kraushaar, U., Zeng, H., et al., 2018. International multisite study of human-induced pluripotent stem cell-derived cardiomyocytes for drug proarrhythmic potential assessment. Cell Rep. 24 (13), 3582–3592. https://doi.org/10.1016/j.celrep.2018.08.079.

Brown, D.A., Perry, J.B., Allen, M.E., Sabbah, H.N., Stauffer, B.L., Shaikh, S.R., Cleland, J.G.F., Colucci, W.S., Butler, J., Voors, A.A., et al., 2017. Mitochondrial function as a therapeutic target in heart failure. Nat. Rev. Cardiol. 14 (4), 238–250. https://doi.org/10.1038/nrcardio.2016.203.

Clements, M., Millar, V., Williams, A.S., Kalinka, S., 2015. Bridging functional and structural cardiotoxicity assays using human embryonic stem cell-derived cardiomyocytes for a more comprehensive risk assessment. Toxicol. Sci. 148 (1), 241–260. https://doi.org/10.1093/toxsci/kfv180.

Davila, J.C., Cezar, G.G., Thiede, M., Strom, S., Miki, T., Trosko, J., 2004. Use and application of stem cells in toxicology. Toxicol. Sci. 79 (2), 214–223. https://doi.org/10.1093/toxsci/kfh100.

Deavall, D.G., Martin, E.A., Horner, J.M., Roberts, R., 2012. Drug-induced oxidative stress and toxicity. J. Toxicol. 2012, 645460 https://doi.org/10.1155/2012/645460.

Doherty, K.R., Wappel, R.L., Talbert, D.R., Trusk, P.B., Moran, D.M., Kramer, J.W., Brown, A.M., Shell, S.A., Bacus, S., 2013. Multi-parameter in vitro toxicity testing of crizotinib, sunitinib, erlotinib, and nilotinib in human cardiomyocytes. Toxicol. Appl. Pharmacol. 272 (1), 245–255. https://doi.org/10.1016/j.taap.2013.04.027.

Durlacher, C.T., Li, Z.L., Chen, X.W., He, Z.X., Zhou, S.F., 2016. An update on the pharmacokinetics and pharmacodynamics of alisertib, a selective aurora kinase a inhibitor. Clin. Exp. Pharmacol. Physiol. 43 (6), 585–601. https://doi.org/10.1111/1440-1681.12571.

FDA, 2001. S7a Safety Pharmacology Studies for Human Pharmaceuticals. https://www.fda.gov/regulatory-information/search-fda-guidance-documents/s7a-safety-pharmacology-studies-human-pharmaceuticals.

FDA, 2005. S7b nonclinical evaluation of the potential for delayed ventricular repolarization (QT interval prolongation) by human pharmaceuticals. https://www.fda.gov/regulatory-information/search-fda-guidance-documents/s7b-nonclinical-evaluation-potential-delayed-ventricular-repolarization-qt-interval-prolongation.

FDA, 2013. FDA requires multiple new safety measures for leukemia drug iclusig; company expected to resume marketing. https://www.fda.gov/drugs/drug-safety-and-availability/fda-drug-safety-communication-fda-requires-multiple-new-safety-measures-leukemia-drug-iclusig.

Fridericia, L.S., 2003. The duration of systole in an electrocardiogram in normal humans and in patients with heart disease. 1920. Ann. Noninvasive Electrocardiol. 8 (4), 343–351. https://doi.org/10.1046/j.1542-474x.2003.08413.x.

Germanguz, I., Sedan, O., Zeevi-Levin, N., Shtrichman, R., Barak, E., Ziskind, A., Eliyahu, S., Meiry, G., Amit, M., Itskovitz-Eldor, J., et al., 2011. Molecular characterization and functional properties of cardiomyocytes derived from human inducible pluripotent stem cells. J. Cell. Mol. Med. 15 (1), 38–51. https://doi.org/10.1111/j.1582-4934.2009.00996.x.

Gills, J.J., Dennis, P.A., 2009. Perifosine: update on a novel akt inhibitor. Curr. Oncol. Rep. 11 (2), 102–110. https://doi.org/10.1007/s11912-009-0016-4.

Green, M.R., Woolery, J.E., Mahadevan, D., 2011. Update on aurora kinase targeted therapeutics in oncology. Expert Opin. Drug Discovery 6 (3), 291–307. https://doi.org/10.1517/17460441.2011.555395.

Guo, L., Coyle, L., Abrams, R.M., Kemper, R., Chiao, E.T., Kolaja, K.L., 2013. Refining the human ipsc-cardiomyocyte arrhythmic risk assessment model. Toxicol. Sci. 136 (2), 581–594. https://doi.org/10.1093/toxsci/kft205.

Hwang, M., Lim, C.H., Leem, C.H., Shim, E.B., 2020. In silico models for evaluating proarrhythmic risk of drugs. APL Bioeng. 4 (2), 021502 https://doi.org/10.1063/1.5132618.

Johannesen, L., Vicente, J., Mason, J.W., Sanabria, C., Waite-Labott, K., Hong, M., Guo, P., Lin, J., Sorensen, J.S., Galeotti, L., et al., 2014. Differentiating drug-induced multichannel block on the electrocardiogram: randomized study of dofetilide, quinidine, ranolazine, and verapamil. Clin. Pharmacol. Ther. 96 (5), 549–558. https://doi.org/10.1038/clpt.2014.155.

Karvelas, G., Roumpi, A., Komporozos, C., Syrigos, K., 2018. Everolimus as cancer therapy: Cardiotoxic or an unexpected antiatherogenic agent? A narrative review. Hell. J. Cardiol. 59 (4), 196–200. https://doi.org/10.1016/j.hjc.2018.01.013.

Kenigsberg, B., Campia, U., Barac, A., 2016. Cardiovascular side effects of cancer treatments. Clin. Pharm. 8 (9) https://doi.org/10.1211/CP.2016.20201651.

Kennedy, M., D'Souza, S.L., Lynch-Kattman, M., Schwantz, S., Keller, G., 2007. Development of the hemangioblast defines the onset of hematopoiesis in human es cell differentiation cultures. Blood. 109 (7), 2679–2687. https://doi.org/10.1182/blood-2006-09-047704.

Khakoo, A.Y., Kassiotis, C.M., Tannir, N., Plana, J.C., Halushka, M., Bickford, C., Trent 2nd, J., Champion, J.C., Durand, J.B., Lenihan, D.J., 2008. Heart failure associated with sunitinib malate: a multitargeted receptor tyrosine kinase inhibitor. Cancer. 112 (11), 2500–2508. https://doi.org/10.1002/cncr.23460.

Lamore, S.D., Ahlberg, E., Boyer, S., Lamb, M.L., Hortigon-Vinagre, M.P., Rodriguez, V., Smith, G.L., Sagemark, J., Carlsson, L., Bates, S.M., et al., 2017. Deconvoluting kinase inhibitor induced cardiotoxicity. Toxicol. Sci. 158 (1), 213–226. https://doi.org/10.1093/toxsci/kfx082.

Lamore, S.D., Kohnken, R.A., Peters, M.F., Kolaja, K.L., 2020. Cardiovascular toxicity induced by kinase inhibitors: mechanisms and preclinical approaches. Chem. Res. Toxicol. 33 (1), 125–136. https://doi.org/10.1021/acs.chemrestox.9b00387.

Lancaster, M.C., Sobie, E.A., 2016. Improved prediction of drug-induced torsades de pointes through simulations of dynamics and machine learning algorithms. Clin. Pharmacol. Ther. 100 (4), 371–379. https://doi.org/10.1002/cpt.367.

Laverty, H., Benson, C., Cartwright, E., Cross, M., Garland, C., Hammond, T., Holloway, C., McMahon, N., Milligan, J., Park, B., et al., 2011. How can we improve our understanding of cardiovascular safety liabilities to develop safer medicines? Br. J. Pharmacol. 163 (4), 675–693. https://doi.org/10.1111/j.1476-5381.2011.01255.x.

Mosquera Orgueira, A., Bao Perez, L., Mosquera Torre, A., Peleteiro Raindo, A., Cid Lopez, M., Diaz Arias, J.A., Ferreiro Ferro, R., Antelo Rodriguez, B., Gonzalez Perez, M.S., Albors Ferreiro, M., et al., 2020. Flt3 inhibitors in the treatment of acute myeloid leukemia: current status and future perspectives. Minerva Med. 111 (5), 427–442. https://doi.org/10.23736/S0026-4806.20.06989-X.

Nerbonne, J.M., Kass, R.S., 2005. Molecular physiology of cardiac repolarization. Physiol. Rev. 85 (4), 1205–1253. https://doi.org/10.1152/physrev.00002.2005.

Nogawa, H., Kawai, T., 2014. Herg trafficking inhibition in drug-induced lethal cardiac arrhythmia. Eur. J. Pharmacol. 741, 336–339. https://doi.org/10.1016/j.ejphar.2014.06.044.

Park, J.S., Jeon, J.Y., Yang, J.H., Kim, M.G., 2019. Introduction to in silico model for proarrhythmic risk assessment under the CiPA initiative. Transl Clin Pharmacol. 27 (1), 12–18. https://doi.org/10.12793/tcp.2019.27.1.12.

Peng, S., Lacerda, A.E., Kirsch, G.E., Brown, A.M., Bruening-Wright, A., 2010. The action potential and comparative pharmacology of stem cell-derived human cardiomyocytes. J. Pharmacol. Toxicol. Methods 61 (3), 277–286. https://doi.org/10.1016/j.vascn.2010.01.014.

Pointon, A., Abi-Gerges, N., Cross, M.J., Sidaway, J.E., 2013. Phenotypic profiling of structural cardiotoxins in vitro reveals dependency on multiple mechanisms of toxicity. Toxicol. Sci. 132 (2), 317–326. https://doi.org/10.1093/toxsci/kft005.

Reimer, K.A., Ideker, R.E., 1987. Myocardial ischemia and infarction: anatomic and biochemical substrates for ischemic cell death and ventricular arrhythmias. Hum. Pathol. 18 (5), 462–475. https://doi.org/10.1016/s0046-8177(87)80031-x.

Saxton, R.A., Sabatini, D.M., 2017. Mtor signaling in growth, metabolism, and disease. Cell 169 (2), 361–371. https://doi.org/10.1016/j.cell.2017.03.035.

Sharma, A., Burridge, P.W., McKeithan, W.L., Serrano, R., Shukla, P., Sayed, N., Churko, J.M., Kitani, T., Wu, H., Holmstrom, A., et al., 2017. High-throughput screening of tyrosine kinase inhibitor cardiotoxicity with human induced pluripotent stem cells. Sci. Transl. Med. 9 (377) https://doi.org/10.1126/scitranslmed.aaf2584.

Strauss, D.G., Gintant, G., Li, Z., Wu, W., Blinova, K., Vicente, J., Turner, J.R., Sager, P.T., 2019. Comprehensive in vitro proarrhythmia assay (CiPA) update from a cardiac safety research consortium / health and environmental sciences institute / FDA meeting. Ther Innov Regul Sci. 53 (4), 519–525. https://doi.org/10.1177/2168479018795117.

Talbert, D.R., Doherty, K.R., Trusk, P.B., Moran, D.M., Shell, S.A., Bacus, S., 2015. A multi-parameter in vitro screen in human stem cell-derived cardiomyocytes identifies ponatinib-induced structural and functional cardiac toxicity. Toxicol. Sci. 143 (1), 147–155. https://doi.org/10.1093/toxsci/kfu215.

Thomas, N., 2012. Innovating pre-clinical drug development: towards an integrated approach to investigative toxicology in human models. In: Paper presented at: AIMBE/NIH Summit on Validation and Qualification of New In Vitro Tools for the Pre-Clinical Drug Discovery Process. NIH.

Valerio Jr., L.G., Balakrishnan, S., Fiszman, M.L., Kozeli, D., Li, M., Moghaddam, S., Sadrieh, N., 2013. Development of cardiac safety translational tools for QT prolongation and torsade de pointes. Expert Opin. Drug Metab. Toxicol. 9 (7), 801–815. https://doi.org/10.1517/17425255.2013.783819.

Wencker, D., Chandra, M., Nguyen, K., Miao, W., Garantziotis, S., Factor, S.M., Shirani, J., Armstrong, R.C., Kitsis, R.N., 2003. A mechanistic role for cardiac myocyte apoptosis in heart failure. J. Clin. Invest. 111 (10), 1497–1504. https://doi.org/10.1172/JCI17664.

William Buchser, P.D., Collins, Mark, Garyantes, Tina, Guha, Rajarshi, Hane, Steven, Lemmon, Vance, Li, Zhuyin, Trask, O. Joseph, 2014. Available from Assay guidance manual [internet]. Bethesda (MD): Eli Lilly & Company and the National Center for Advancing Translational Sciences [accessed July 6th 2021]. https://www.ncbi.nlm.nih.gov/books/NBK100913/.

Woosley, et al., 2021. Qtdrugs list. AZCERT, Inc.. www.CredibleMeds.org

Yang, L., Soonpaa, M.H., Adler, E.D., Roepke, T.K., Kattman, S.J., Kennedy, M., Henckaerts, E., Bonham, K., Abbott, G.W., Linden, R.M., et al., 2008. Human cardiovascular progenitor cells develop from a kdr+ embryonic-stem-cell-derived population. Nature. 453 (7194), 524–528. https://doi.org/10.1038/nature06894.

Zhang, D., Shadrin, I.Y., Lam, J., Xian, H.Q., Snodgrass, H.R., Bursac, N., 2013. Tissue-engineered cardiac patch for advanced functional maturation of human esc-derived cardiomyocytes. Biomaterials. 34 (23), 5813–5820. https://doi.org/10.1016/j.biomaterials.2013.04.026.

Zhao, H., Chen, G., Liang, H., 2019. Dual pi3k/mtor inhibitor, xl765, suppresses glioblastoma growth by inducing er stress-dependent apoptosis. Onco. Targets Ther. 12, 5415–5424. https://doi.org/10.2147/OTT.S210128.